Molecular Structure Characterization of Hyperbranched Polyesteramides

Erik T. F. Geladé,* Bart Goderis, Chris G. de Koster, Nico Meijerink, and Rolf A. T. M. van Benthem

DSM Research, P.O. Box 18, 6160 MD Geleen, The Netherlands

Roel Fokkens and Nico M. M. Nibbering

Institute of Mass Spectrometry, University of Amsterdam, Nieuwe Achtergracht 129, 1018 WS Amsterdam, The Netherlands

Kell Mortensen

Condensed Matter Physics and Chemistry Department, Risø National laboratory, DK-4000 Roskilde, Denmark

Received July 20, 2000; Revised Manuscript Received December 18, 2000

ABSTRACT: The molecular structure of a series of hyperbranched polyesteramides was studied using size exclusion chromatography (SEC), mass spectrometry (MS) and small-angle neutron scattering (SANS). Products with increasing molecular mass were obtained through the polycondensation of in situ produced AB_2-like monomeric units. Electrospray ionization MS indicates that narrow SEC fractions consist of different isomers, the number of which increases with molecular mass. Molecular mass moments and polydispersity numbers increase with polycondensation degree. The SANS measurements and SEC−DV data yield values for the polymers fractal dimension, which can be rationalized in the framework of percolation theory that originally was designed for randomly branched polymers. Randomly branched polymer behavior in this particular case possibly results from a side reaction involving reactivity among B-end groups.

Introduction

Hyperbranched polymers (HPs) are a relatively new type of highly branched materials, which—in contrast to dendrimers—often are prepared via a one-step synthesis.[1] Their molecular architecture is not as well-defined as for dendrimers and their molecular mass distribution is not monodisperse, giving rise to different properties. For example, dendrimers display a maximum in the relationship between their intrinsic viscosity and molecular mass, while in general HPs do not.[2] An exception can be found in work by Hobson and Feast[3] reporting dendrimer-like behavior for HPs as well.

HPs also differ from randomly branched chains. The latter can be considered as reaction products of multifunctional (A_n) monomers, having "*n*" active "A" groups, which are able to react with each other with equal probability. In addition, this probability does not change if the functional group is connected to a growing chain by an earlier reaction.[4,5] Randomly branched polymers are characterized by an extremely broad molecular mass distribution and can be described either by Flory−Stockmayer theory[6,7] or percolation theory.[8,9] Theory predicts gelation at a critical point in the reaction.[4,5,10,11]

Hyperbranched structures are also made from multifunctional monomers but their monomeric units have at least two *different* chemical functionalities with the constraint that—e.g., in the case of AB_2 units—"A" can only react with "B". In principle, this gives rise to narrower molecular mass distributions compared to randomly branched products and the advantage that gelation can never occur.[10] The hyperbranched polymers (Hybrane) discussed in the present paper are condensation products of 1,2-cyclohexanedicarboxylic anhydride (C) with di-2-propanolamine (DIPA, abbreviated as D). The first (fastest) reaction is the formation of an amide bond resulting in an AB_2 monomeric unit (with "A" carboxylic acid and "B" alcohol groups). The following reactions are esterifications giving rise to hyperbranched structures. However, in the accompanying paper by van Benthem et al.,[12] a side reaction is mentioned of the 2-hydroxypropylamide end groups. These end groups react with secondary amines that are present in the polycondensation mixture either as unreacted DIPA or as a result of an acyl shift of the hydroxy-propylamides themselves. The reaction involving the latter gives rise to chain extension and a strong increase of the higher moments of the molecular mass distribution, especially for reactions that are initiated from mixtures with little excess DIPA, that is at a low D/C ratio. In fact, this side reaction represents the unwanted reactivity among B groups in this AB_2-type polycondensation. As a result, such reaction mixtures display random copolymer behavior at a sufficiently low D/C ratio, i.e., gelation. In view of this side reaction the present hyperbranched polyesteramides cannot be considered as representatives for other (side reaction free) AB_2-based hyperbranched molecules.

The theoretical aspects of hyperbranched polymers were treated first by Flory[13a] and later by Burchard.[13b] Cyclization reactions were not accounted for although they have been clearly monitored by NMR spectroscopy and MALDI−TOF (matrix-assisted laser desorption/ionization-time-of-flight) MS (mass spectrometry).[14]

Molecular mass distributions (MMDs) are in general determined by size exclusion chromatography (SEC).

* To whom correspondence should be addressed.

10.1021/ma001266t CCC: $20.00
Published on Web 04/27/2001

For HPs, a conventional calibration based on linear reference standards and a concentration detector for sure is not appropriate. Relying on the pioneering work by Grubisic et al.,[15] who studied a very broad range of different linear and branched polymers, one may apply the so-called universal calibration, involving viscometric detection in addition to concentration detection (SEC−DV). Mourey et al.[16] demonstrated that this method works reasonably well in the case of polyether mono- and tridendrons. They also discuss the possibility of deviations from the universal calibration with increasing dendrimer generation. These deviations are, however, small. Patton et al.[17] did not use SEC−DV but exploited the principle of universal calibration and obtained quite consistent results in the case of randomly branched polyesters over a wide molecular mass range. Kim and Webster[18] claim that the absolute molecular mass of a HP can be obtained by using universal calibration but that it is not legitimate to use only SEC for a complete structural analysis of HPs due to geometrical isomerism. The latter refers to structural differences for molecules with identical molecular mass.

A detailed molecular characterization of HPs is rather difficult. The degree of branching is often determined via NMR or IR spectroscopy yielding typically degrees of branching between 15 and 90%.[19] Recently, however, it has been shown that the degree of branching is not an adequate descriptor for the shape of dendritic molecules.[2b] In that respect it is of interest to consider MALDI−TOF−MS as an alternative. This technique allows for a good structural identification of the HPs involving chemical composition and end group composition determination as a function of molecular mass.[20] Provided the MMD of the samples is suficiently narrow, MALDI spectra also yield values for the molecular mass. Because of current instrumental limitations and experimental parameters MALDI does not provide realistic estimates of the MMD in the case of polydisperse samples.[20] In that case there is a disagreement between the MMD obtained by MALDI−TOF−MS and the distribution provided by SEC.[20] Particularly, detector saturation leads to discrimination of the high mass-tail of molecular mass distributions when the polydispersity exceeds 1.2. These limitations can be overcome by coupling SEC to MALDI. The molecular masses calculated from the MALDI spectra of narrow SEC fractions ($M_w/M_n < 1.2$) can be used to check the validity of the universal calibration.

The solution structure of HPs can also be studied using small-angle X-ray (SAXS) and neutron (SANS) scattering.[21] In this work on hyperbranched polyesteramides a combination of SEC−viscometry, SEC−mass spectrometry (MS), and SANS is used. The results are discussed in the framework of percolation theory prediction.

Experimental Section

Materials. Five samples with increasing molecular mass—obtained by varying the D/C ratio—were studied (Table 1). Attempts to synthesize higher molecular masses (by using even lower D/C ratios) end up in gelation. Details about the synthesis and the chemical characterization of the materials can be found in the accompanying paper.[12]

Methodology. SEC. The SEC experiments were performed on a Hewlett-Packard chromatograph (HP 1090) equipped with a differential refractometer (RI) and a differential viscometer (DV) placed in parallel (Viscotek 200).

Table 1. Chemical Composition Information of Studied Hybrane Resin Samples, Where C = Cyclohexanediacic Anhydride and D = dipa (Di-2-propanolamine)

	no of moles			
sample	C	D	D/C	exptl convn
1	2.108	3.108	1.47	0.988
2	2.947	3.947	1.35	0.988
3	4.005	5.005	1.26	0.988
4	5.321	6.321	1.20	0.984
5	6.941	7.941	1.14	0.989

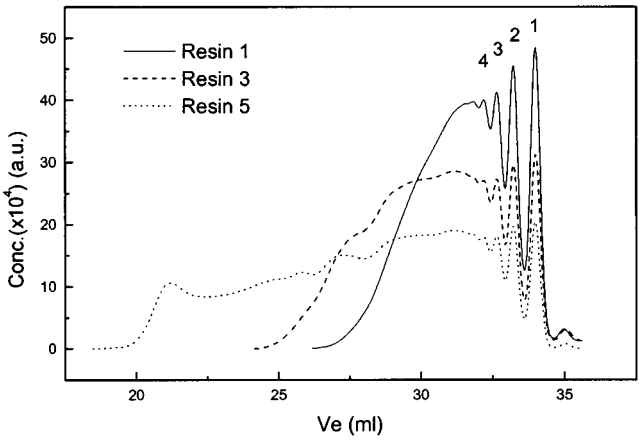

Figure 1. Typical SEC concentration chromatograms using a refractive index detector. The area under the chromatogram is equal to 74 ± 1 mV·mL·mg^{-1} for each sample These curves were scaled to cover an (arbitrary) area of 10000 (hence a.u. in the ordinate axis).

The Hybrane resins were dissolved in dichloromethane (p.a. Merck) at room temperature in a nitrogen atmosphere for a few hours. All polymer solutions were filtered using Millex filters (pores size 0.5 μm). Four Polymer Laboratories (PL) mixed C columns were applied. The eluent was degassed using a degasser (PL-DG 802). To avoid adsorption and repulsion effects, triethylamine was added to the solvent/eluent (0.1 M). The solvent flow rate was 1 mL·min^{-1}. The injection volume was 200 μL. Measurements were done at 23 ± 1 °C. Under these conditions, the chromatograms are reproducible. At high retention times the low molecular mass peaks of different samples overlap very well as expected from the chemistry (Figure 1).

From both the concentration and viscosity chromatograms, the intrinsic viscosity [η] as a function of elution volume was determined. From these data the molecular mass distribution (MMD) and the moments (M_n, M_w, and M_z) were calculated using the universal calibration[15] with polystyrene standards obtained from PL with known molecular masses in the range between 580 and 2 850 000 g·mol^{-1}. All data were processed using Trisec 2.70 software (Viscotek). In addition the constants K and a were extracted from a plot of log[η] vs log(M) by linear regression, based on the Mark−Houwink equation:

$$[\eta] = KM^a \tag{1}$$

SEC−MALDI−TOF−MS. Fractions of sample 2 were collected during a SEC run for off-line MALDI−TOF spectrometry (MS). The sampling time per fraction was 12 s, which is equivalent to 0.2 mL of eluent. The volume offset between the starting point of each fraction and the corresponding RI signal was determined by placing a UV detector behind the RI detector at the fraction collector starting point. The offset volume is determined using a PS calibration standard (molecular mass 19 000 g mol^{-1}).

The as obtained SEC fractions were diluted for MALDI−TOF−MS by adding 100 μL of tetrahydrofuran (THF). Next, 10 μL of the latter solution was mixed with 30 μL of a solution of 3 mg/L 2,5-dihydroxybenzoic acid in THF. One microliter

of that solution was loaded on the gold−sample plate. Finally, THF was removed by evaporation in warm air.

MALDI−TOF−MS was carried out using a Perkin-Elmer/Perseptive Biosystems Voyager-DE-RP MALDI−TOF mass spectrometer [Perseptive Biosysytems, Inc., Framingham, MA] equipped with delayed extraction.[22] A 337 nm UV nitrogen laser producing 3 ns pulses was used, and the mass spectra were obtained in the linear and reflectron modes. The MALDI−TOF−MS spectra were processed to yield values for M_n and M_w.[23] The polydispersity (M_w/M_n) of a fraction typically is 1.02. The calculated molecular masses via MALDI−TOF−MS were correlated to the SEC elution volume but additionally corrected for by 0.1 mL since each SEC fraction has a volume of 0.2 mL.

SEC−ESI−MS. Similar SEC fractions of sample 1 were studied by positive ion electrospray (ESI) mass spectrometry (MS) using a PE Sciex API 150 single quadrupole mass spectrometer [Perkin-Elmer Sciex, Toronto, Ontario, Canada]. The fractions were introduced through the electrospray interface by infusion of a THF solution containing 20 mM sodium iodide at 5 μL min^{-1} with a syringe pump [Harvard Apparatus, Saint Laurent, Quebec, Canada]. Nitrogen was used as nebulizing and curtain gas. NaI was added to enhance the ionization of the oligomers. Electrospray of the samples under these conditions leads to the formation of single to multiple sodium cationized $[M + nNa]^{n+}$ molecules. The charge state of the cationized oligomers depends on the molecular mass and the sodium iodide concentration. The strategy used for the identification of the sodium cationized oligomers and for determination of the chemical composition of the individual oligomers by extrapolation to zero oligomers has been discussed elsewhere.[24,25] This strategy has been applied here without any modification. The capillary tip was maintained at 5 kV, while the orifice was set at 30 V. Mass spectra were collected in full scan mode, scanning from m/z 100−2000 Da in 30 s. The mass spectral data were processed with the MultiView 1.4 software [PE Sciex].

SANS. The small-angle neutron scattering (SANS) experiments were performed at the SANS facility of the Risø National Laboratory, Roskilde, Denmark. Three different setups were selected: (1) $\lambda = 3$ Å, $D = 1$ m; (2) $\lambda = 3$ Å, $D = 3$ m; (3) $\lambda = 6$ Å, $D = 6$ m (λ = wavelength, D = sample-to-detector distance). The scattering data were all azimuthally isotropic and were therefore radially averaged to provide the $I(q)$ scattering function, where $q = (4\pi/\lambda)\sin(\theta)$ is the scattering momentum and 2θ the scattering angle. The raw data were corrected for absorption, solvent scattering, and experimental background and, for the 3 Å-setting data sets, were converted into absolute units using water as a secondary standard, according to standard procedure. The 6 Å/6 m-data set was calibrated using a least-squares fitting procedure to overlap with the 3 Å/3 m-data set. Solutions of 1% (m/m) polymer in tetrahydrofuran-d_4, THF-d_4, were measured in 2 mm-thick quartz cuvettes. This concentration proved to be the optimal concentration with respect to the scattered intensity and negligible interparticle interference effects. Using CD_2Cl_2 as a solvent would have been better for consistency with the SEC−DV results, but this was not an option because of too high an absorption. Cl-containing products (as, e.g., CD_2Cl_2) are known to absorb neutrons quite strongly. THF was not an option for SEC because of strong adsorption effects.

In general scattering intensity curves of polymer solutions, $I(q)$, consist of scattering contributions from the molecular shape, $P(q)$, and intermolecular interference, $S(q)$, i.e., $I(q) \cong P(q)S(q)$. For dilute polymer concentrations in noninteracting systems $S(q) = 1$. The z-average radius of gyration, R_{gz}, was extracted from the scattering patterns by linear regression in a so-called Zimm plot, which is a plot of $1/I(q)$ vs q^2 according to[26−29]

$$P_{\text{Zimm}}(R_{gz}, q) = C/\left(1 + \frac{q^2 R_{gz}^2}{3}\right) \tag{2}$$

where C is a constant, to be taken into account for intensities that are scaled arbitrarily. For samples 1−3, the 6 Å/6 m data set was not taken into account because of a too high noise level. No R_{gz} value could be obtained for samples 4 and 5 because the required q range for such analysis given by the condition $qR_{gz} \ll 1$ is outside the experimental window. The sample−detector distance (6 m) could not be increased, and selecting a higher wavelength would have lowered the neutron flux considerably leading to extremely long measuring times.

For polymers that can be characterized as (mass) fractals within a given length scale and with an effective fractal dimension, $d_{f,eff}$, the scattering function is given by

$$P_{\text{fractal}}(q) = q^{-d_{f,eff}} \tag{3}$$

within the corresponding q-regime. This q-region where a fractal concept holds is at low q determined by the overall polymer size, and at high q by the polymer statistical segment length l, i.e., $1/R_{gz} < q < 1/l$. To obtain meaningful estimates for $d_{f,eff}$, the region of linearity in a double logarithmic plot of $I(q)$ vs q should be at least 1 decade.[28,30] As will be shown below, this is only the case for sample 5. Nevertheless, an estimate of $d_{f,eff}$ was extracted in a narrower q range for samples 3 and 4. Such analysis for samples 1 and 2 was considered meaningless.

Fractal Dimension. The concept of fractals has been introduced by Mandelbrot.[31] A three-dimensional object (Euclidean dimension) with the same density throughout has a mass fractal dimension of 3. This means that the amount of material (the mass, M) enclosed by an imaginary sphere with its center in the center of the object increases with a power 3 as the radius of the sphere (R) increases, that is $M \sim R^3$. The mass enclosed by a similar sphere in the case of a thin rod increases linearly with the increase of R, i.e., $M \sim R^1$, and obviously, the rule for a platelike structure is $M \sim R^2$. The mass of polymers in solution usually increases with a noninteger (fractal) power, d_f,. of the radius. This implies that the polymer segment density is not constant but changes (usually decreases) in a well-defined manner with increasing R. The better the solvent the more expanded a polymer coil is and the lower the corresponding d_f. For linear polymer coils $d_f = {}^5/_3$ or 2 for a good or a Θ solvent, respectively. Branching usually increases d_f with respect to that of its linear counterpart. According to theory, randomly branched polymers are characterized by $d_f = 2$ in a good solvent or $d_f = 2.28$ in a Θ solvent.[4,5,10] Occasionally a fractal dimension of 3 was obtained for dendrimers,[32] indicative for a homogeneous polymer segment distribution.

The fractal dimension of monodisperse polymers can be extracted directly from the angular dependence of the scattered light or neutron intensity in the intermediate q range as discussed above (eq 4 with $d_f = d_{f,eff}$). Alternatively—and parallel to the descriptive explanation given above—d_f can also be obtained from the molecular mass (M) dependence of the radius of gyration (R_g) since

$$R_g \sim M^{1/d_f} \tag{4}$$

Using the Mark−Houwink exponent a, d_f can also be derived according to[33]

$$d_f = \frac{3}{1 + a} \tag{5}$$

The fractal dimension, d_f, is not affected by polydispersity, provided it is not exessively high. However, Daoud et al.[34] considered randomly branched polymers, which have an extremely broad molecular mass distribution and showed that in this particular case the experimentally observed value for $d_{f,eff}$ is affected by the very high degree of polydispersity. Below, it will be demonstrated that the concepts of Daoud et al.[34] for randomly branched structures can also be applied to our hyperbranched polyesteramides.

The measured fractal dimension of such unfractionated, highly polydisperse samples is an *effective* fractal dimension

Table 2. Molecular Parameters As Obtained Using SEC−DV, Where Molecular Mass Distribution Moments Are Expressed in g/mole

sample	M_n	M_w	M_z	M_w/M_n	M_z/M_w	$[\eta]_0$ (dl/g)
1	1500	3600	7900	2.3	2.2	0.045
2	1800	5900	16 000	3.3	2.7	0.050
3	2400	11 000	33 000	4.5	3.1	0.057
4	2400	59 000	391 000	25	6.6	0.100
5	2800	248 000	1 730 000	87	7.0	0.130

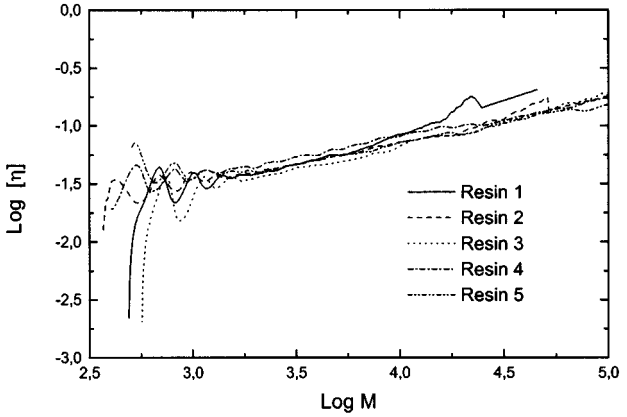

Figure 2. Mark−Houwink plots of all resins. To obtain the Mark−Houwink constants, a linear regression was performed over the entire molecular mass range depicted.

$d_{f,eff}$ [34] and is related to the real fractal dimension d_f according to

$$d_f = \frac{d_{f,eff}}{3 - \tau} \tag{6}$$

with τ a critical polydispersity exponent[35] which was predicted by Flory[6] and Stockmayer[7] to be equal to 2.5 and by percolation theory[8,9] to 2.2. Earlier experiments point to a preference for the percolation model over the Flory−Stockmayer model.[17,36] Daoud et al.[34] further deduced the two following relations which in combination can be used to find the two unknown parameters d_f and τ

$$R_{gz} \sim M_w^{1/d_{f,eff}} = M_w^{(3-\tau)/d_f} \tag{7}$$

$$[\eta]_0 \sim M_w^{((3/d_f)-\tau+1)/(3-\tau)} \tag{8}$$

with $[\eta]_0$ the bulk intrinsic viscosity of the unfractionated sample. Alternatively, τ can be obtained from the SEC moments directly using

$$M_w \sim M_z^{(3-\tau)} \tag{9}$$

a relation which is based on original ideas by Leibler and Schosseler[36] and which has been used successfully in the past.[17,33,38]

Results and Discussion

Molecular Mass Distributions, Moments and Intrinsic Viscosities from SEC−DV. In Table 2, SEC−DV based molecular mass moments and bulk intrinsic viscosities ($[\eta]_0$) are presented.

The molecular masses, intrinsic viscosities as well as the polydispersity indices (M_w/M_n and M_z/M_w) increase with decreasing D/C. A broad molecular mass distribution and an increasing M_z/M_w with increasing M_w are characteritics of randomly branched polymers while on the contrary for HPs a constant M_z/M_w is predicted by Burchard.[33] Figure 2 illustrates the Mark−Houwink plots of the different resins.

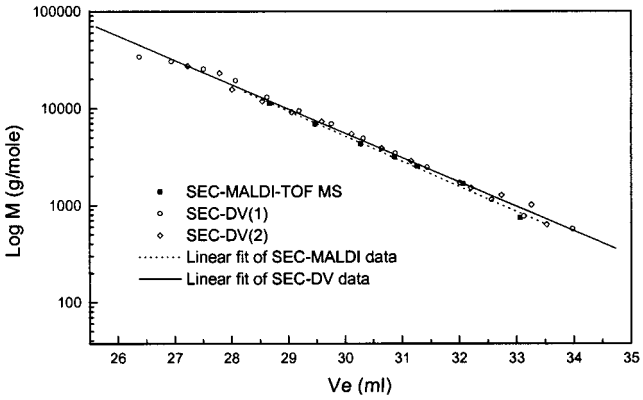

Figure 3. Logarithmic plot of molecular mass (from SEC−DV and MALDI−TOF−MS) as a function of elution volume V_e.

The slope which is the Mark−Houwink constant a is between 0.3 and 0.4 for all samples and is typical for hyperbranched polymers.[19]

All these values are only meaningful if the universal calibration principle is valid. As there has been no report stating that it is not the case for HPs and relying on literature in which the universal calibration principle was applied successfully to other branched polymers[16−18] (dendrimers and randomly branched polymers) we feel confident that this principle also holds in the case of HPs. Moreover, there is independent proof for molecular masses below 10000, which is discussed next.

Molecular Masses of SEC Fractions from MS. The MALDI−TOF−MS based molecular masses obtained for the fractions of sample 2 are illustrated in Figure 3. These values are compared to the SEC−DV data of the samples 1 (DV(1)) and 2 (DV(2)). Since the molecular mass in SEC−DV for each slice corresponds to the number-average molecular mass,[39] comparison with the number-average molecular masses from MS is made. The MS and SEC−DV values agree very well. Also on a linear y-scale the differences are small, indicating that for these HPs the universal calibration can very well be applied, at least below a molecular mass of 10000. This confirms earlier results by Jahromi et al.[40] for side chain dendritic polymers having a backbone with pending monodendrons.

Chemical Composition of SEC Fractions from MS. A typical ESI−MS spectrum of a SEC fraction of sample 1 is given in Figure 4. It is composed of two charge distributions: a charge distribution of triply charged ions between m/z 950 and 1600 and a distribution of doubly charged ions between m/z 1400 and m/z 2200.

Three series of structurally related homologous oligomers are present in the upper panel of the ESI-MS spectrum in Figure 4. The labeled peaks at m/z 965, 1055, 1144, 1234, 1324, and 1411 are associated with the cationization by three sodium cations, that is C_nD_{n+1} $[M + 3Na]^{3+}$ ions. The second series of peaks at m/z 1002, 1091, 1181, 1271, 1361, and 1451 is assigned to $[M + 3Na]^{3+}$ C_nD_{n+2} oligomers and finally the peaks at m/z 1099, 1189, 1278, and 1368 originate from triply sodiated cyclic $C_nD_n-H_2O$ oligomers. Other peaks in the ESI spectrum are the result of ionization by a proton and two sodium cations $[M + 2Na + H]^{3+}$ and $[M + Na + 2H]^{3+}$, or by three protons, $[M + 3H]^{3+}$.

The lower panel shows similar results for the doubly charged oligomers. An interesting observation in this

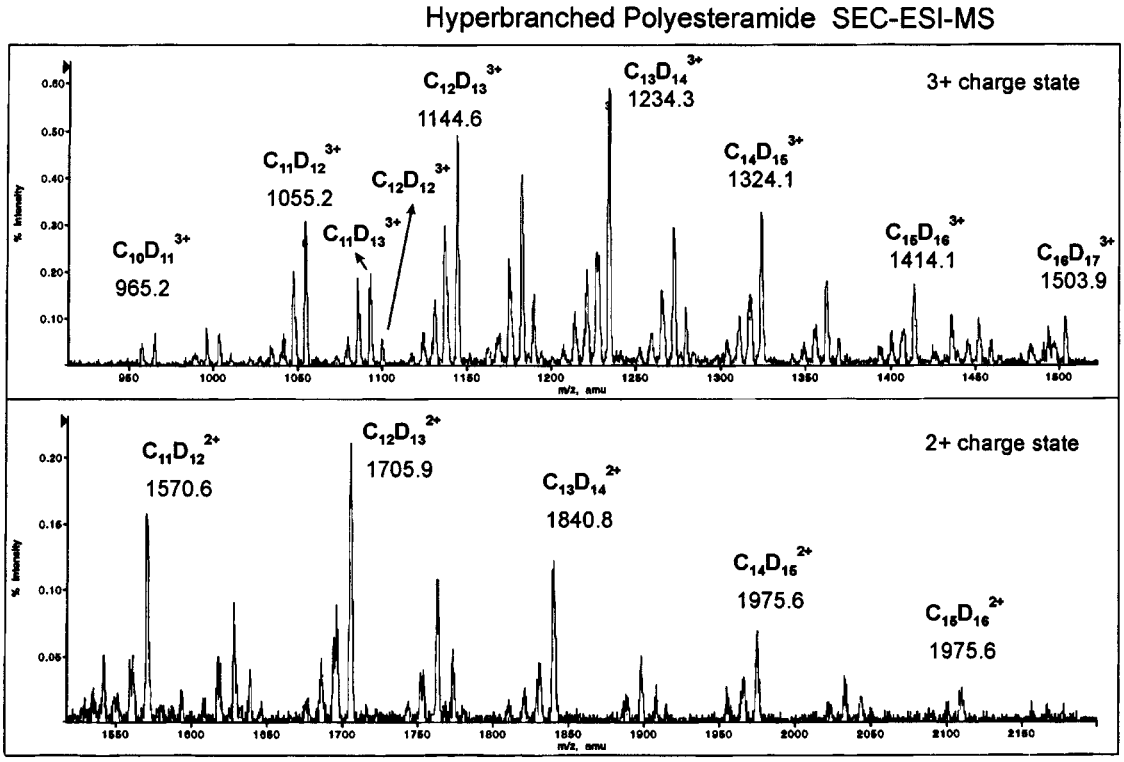

Figure 4. ESI−MS spectrum of the SEC fraction at elution volume of 32 mL for sample 2.

ESI study is that small SEC fractions are required to generate pseudomolecular $[M + nNa]^{n+}$ ions of the higher molecular mass oligomers. These signals are absent in the ESI spectrum of an unfractionated sample. In summary, the ESI spectrum shows a complex chemical composition and end group distribution. These distributions are mainly composed of three series of homologous oligomers C_nD_{n+1}, C_nD_n, and C_nD_{n+2}.

The ESI mass spectra were used to assign the oligomeric peaks (1−4) in the SEC chromatogram (Figure 1) and to study the chemical composition as a function of molecular mass. From the electrospray spectra (data not shown), it is evident that peak 1 is composed of three different oligomers. The main constituent is the CD_2 oligomer. Minor contributions to the SEC concentration detector signal at this elution volume come from the CD_3 and to a lesser extent the C_2D_2 oligomer. The maxima of the CD_2, CD_3, and C_2D_2 contributions do not coincide. The maximum of the latter is shifted toward the minimum between peaks 1 and 2. Peak 2 originates mainly from the C_2D_3 oligomer with some contributions from the C_2D_4 and C_3D_3 oligomers. Similarly, peaks 3 and 4 are composed out of the higher homologues of the C_nD_{n+1}, C_nD_n, and C_nD_{n+2} oligomers. From the ESI measurements it is evident that the oligomeric peaks in the SEC chromatogram are composed out of three oligomeric series. The most abundant one is the C_nD_{n+1} series. It is obvious that the oligomeric peaks in the SEC chromatogram are chromatographically not pure. Thus, the maxima of these peaks cannot be used to check the quality of the universal calibration. From the present ESI results it became also clear that the C_nD_{n+1}, C_nD_n and C_nD_{n+2} composition of the SEC slices builds up regularly as a function of their M_n; i.e., n increases as a function of the SEC fraction number. This implies that the increasing number of isomers at higher molecular masses due to more modes for branching does not lead to a great variation in hydrodynamic volumina.

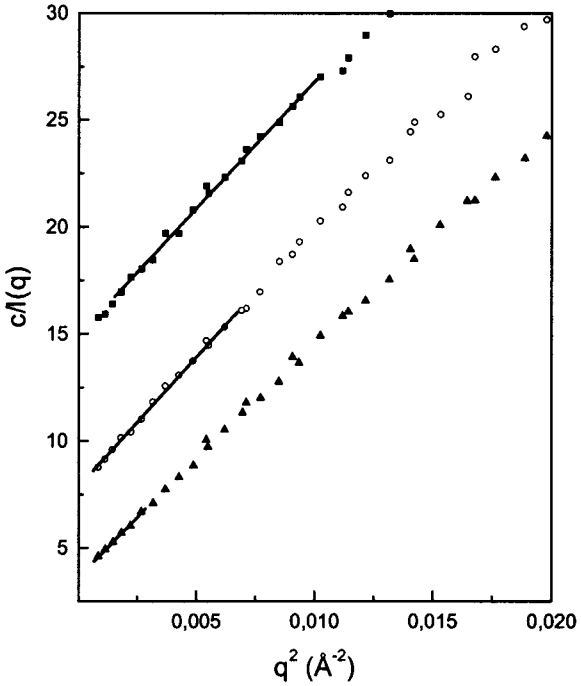

Figure 5. Zimm plots (resin 1, solid squares; resin 2, open circles; resin 3, solid up triangles). The actual fitting ranges are highlighted with the straight lines that were used to determine R_{gz}.

Radii of Gyration. SANS based Zimm plots are shown in Figure 5. Thick full lines, representing the results of the linear regression, highlight the q ranges actually used to determine R_{gz}. These ranges and the obtained R_{gz} values are included in Table 3.

Fractal Dimension. So far three elements were highlighted that point to randomly branched polymer

Table 3. R_{gz} Values for the Different Samples Obtained by Using the Zimm Approach[a]

sample	M_w (g/mol)	R_{gz} Zimm (Å)	q range (Å^{-1})
1	3600	15.5 ± 0.3	0.047−0.092
2	5900	21.6 ± 0.3	0.034−0.079
3	11 000	30.5 ± 0.7	0.030−0.052
4	59 000	n.a.	
5	248 000	n.a.	

[a] The q ranges in which the analysis was performed are indicated. n.a.: not available.

Table 4. Mark−Houwink Constant a and the Fractal Dimension d_f as Calculated from SEC−DV results

sample	M_w	a	d_f
1	3600	0.35−0.5	2.22−2
2	5900	0.37	2.19
3	11 000	0.34	2.24
4	59 000	0.34	2.24
5	248 000	0.33	2.26

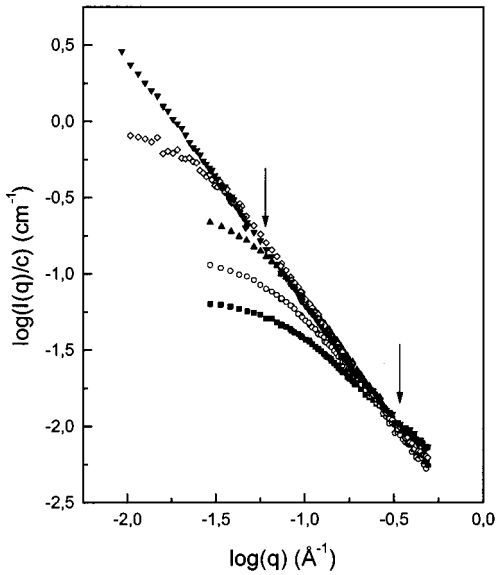

Figure 6. Double logarithmic presentation of the scattering patterns (resin 1, solid squares; resin 2, open circles; resin 3, solid up triangles; resin 4, open diamonds; resin 5, solid down triangles). The intensities were normalized to the concentration c (expressed as mass %). Arrows indicate the edges of the fractal region for sample 4.

behavior for the present HPs: (1) gelation occurs under certain conditions, (2) the molecular mass distributions are very broad, and (3) the M_z/M_w ratio increases with increasing M_w. For that reason, we treated our data in terms of theories that were developed originally for randomly branched polymers. First, the polydispersity exponent, τ, was calculated from a double logarithmic plot of M_w vs M_z according to eq 9. The result is 2.23 ± 0.03 if all samples are taken into account and 2.22 ± 0.05 if only the three lowest M_w samples are considered (for which the universal calibration is proofed). These τ values are identical within experimental error. They are below the values found experimentally for other randomly branched polyesters[17,33,38] but are in good agreement with the prediction from percolation theory.[8,9]

The method involving eq 5 and the Mark−Houwink constant a directly yields d_f values for the HPs in CH_2Cl_2. The results are collected in Table 4 and are between the predictions for randomly branched polymers in a good solvent (2) and a Θ solvent (2.28). There are no significant differences between the d_f values of samples 2−5, indicating that the degree of branching and/or solvent−polymer compatibility does not change significantly by changing the reaction conditions, that is the D/C ratio. The degree of branching or solvent−polymer compatibility also does not change significantly with increasing M, which can be deduced from the single and constant slopes in Figure 2. Sample 1, however, behaves differently. The slope of the latter in a Mark−Houwink plot (which is Figure 2) clearly increases with increasing molecular mass. For that reason a range of fractal dimensions is given in Table 4. This curvature may point to a decrease of branching with increasing M for this particular sample (assuming the polymer solvent interaction to be independent of M). This behavior has been found more often[19] for HPs and does not agree with theoretical calculations.[2]

Table 5. SANS-Based Effective and Real Fractal Dimensions for the Different Samples[a]

sample	M_w	$d_{f,eff}$	d_f	q range (Å^{-1})
1	3600	n.d.		
2	5900	n.d.		
3	11 000	1.63 ± 0.01	2.02 ± 0.01	0.14−0.35
4	59 000	1.68 ± 0.01	2.08 ± 0.01	0.08−0.3
5	248 000	1.630 ± 0.006	2.030 ± 0.007	0.03−0.3

[a] In the last column, the q range used for the determination of $d_{f,eff}$ is indicated. n.d.: not determined.

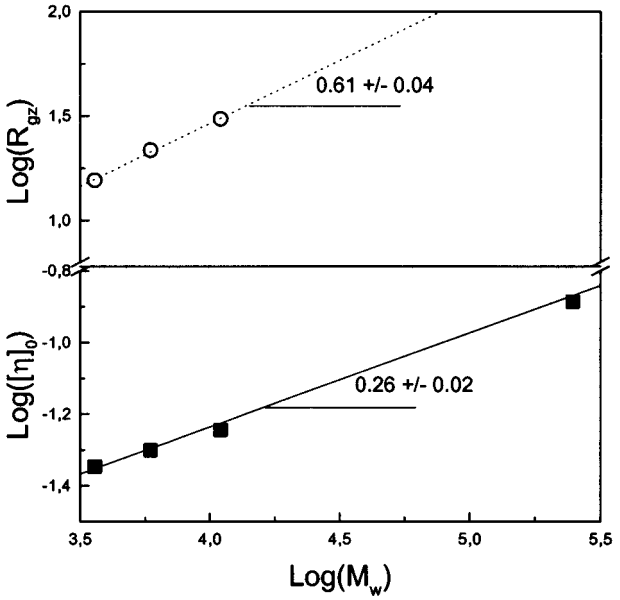

Figure 7. Double logarithmic representation of R_{gz} vs M_w and $[\eta]_0$ vs M_w. The slopes equal 0.61 and 0.26, respectively.

The linear region in a double logarithmic plot of $I(q)$ vs q (Figure 6), proofs the fractal behavior of the present HPs. This linearity is particularly clear in the case of sample 5. Effective fractal dimensions were extracted from this figure and the theorethical percolation value for τ (2.2) was used to convert these (THF-d_4) $d_{f,eff}$ estimates into d_f values. This τ value was selected because the values obtained above are within experimental error not different from the theoretical prediction. All results are collected in Table 5.

The values for d_f in Table 5 point to THF-d_4 being a good solvent. No $d_{f,eff}$ values can be obtained for the low molecular mass samples allong this route. However, for these particular samples R_{gz} values are available, which in combination with the SEC-based M_w data can be used to determine a $d_{f,eff}$ according to eq 7. The slope in a double logarithmic plot of R_{gz} vs M_w yields $1/d_{f,eff}$ as

illustrated in the top image of Figure 7. The resulting $d_{f,eff}$ equals 1.67 ± 0.8 and is identical to the values obtained above for the higher molecular mass samples.

As explained in the Experimental Section, τ as well as d_f can be calculated by solving the eqs 7 and 8. The slope in a double logarithmic plot of $[\eta]_0$ vs M_w equals 0.26 ± 0.02 which in combination with the slope in a similar plot of R_{gz} vs M_w (Figure 7) yields a value for τ of 2.21 ± 0.04 and for d_f of 2.11 ± 0.04. The value of τ once again is in agreement with percolation theory and the d_f value is between that of the HPs in CH_2Cl_2 and THF-d_4. Note that the as obtained values for τ and d_f are "hybrid" values since the R_{gz} estimates are based on SANS measurements in THF-d_4 whereas the $[\eta]_0$ data were determined in CH_2Cl_2.

Conclusions

To characterize the molecular structure of hyperbranched polyesteramides the combination of SEC, MS and SANS proved to be very strong. It could be concluded that the present HPs behave like randomly branched polymers in different aspects.

At lower D/C ratio than the ones reported here, gelation occurs. The molar mass distributions are extremely broad and the ratio M_z/M_w is not constant but increases with the molar mass of the polymer, which is not expected for (true) AB_2 systems but which is a characteristic of randomly branched polymers. Using concepts that were originally designed for randomly branched polymers the SEC−DV and SANS data could be rationalized satisfactorily. The fractal dimension of the HPs in CH_2Cl_2 extracted from Mark−Houwink plots is between the values predicted for randomly branched polymers in good solvents and Θ solvents, respectively. A 'percolation like' τ value could be extracted from the SEC based M_w and M_z data. Using the three lowest molecular mass samples an effective fractal dimension could be derived for the HPs in THF-d_4 using the SANS based R_{gz} data in combination with the SEC-based M_w values. This value is identical to the prediction for randomly branched polymers in a good solvent. The SANS-based effective fractal dimension of the highest molar mass samples in THF-d_4 based on the slope of the intensity curves in a double logarithmic plot is identical to the value obtained along a different route for the lower molecular mass samples.

Despite the very good compatibility of the present data with percolation theory predictions for randomly branched polymers it cannot be claimed at this stage that all AB_2-based HPs behave in a similar way because of a side reaction in the present case involving reactivity between B end groups.

Some of the conclusions rely on the validity of the universal calibration principles, which could be proofed for molecular masses below 10 000 by combining SEC with MALDI−TOF−MS. ESI−MS in combination with SEC showed that all SEC fractions consist of several isomers, the number of which increases with increasing molecular mass.

Acknowledgment. The management of DSM Research, DSM Coating Resins, and DSM New Business Development is kindly acknowledged for permission to publish this work.

References and Notes

(1) Fréchet, J. M. J.; Hawker, C. J.; Gitsov, I.; Leon, J. W. *Pure Appl. Chem.* **1996**, *A33*, 1399.
(2) (a) Aerts, J. *Comput. Theor. Polym. Sci.* **1998**, *8* (1/2), 49. (b) Widmann, A. H.; Davies, G. R. *Comput. Theor. Polym. Sci.* **1998**, *8* (1/2), 191.
(3) Hobson, L. J.; Feast, W. J. *Chem. Commun.* **1997**, *21*, 2067.
(4) Isaacson, J.; Lubensky, T. C. *J. Phys. Lett.* **1980**, *41*, L469.
(5) Daoud, M.; Joanny, J. F. *J. Phys. (Les Ulis, Fr.)*, **1981**, *42*, 1359.
(6) Flory, P. J. *J. Am. Chem. Soc.* **1941**, *63*, 3083, 3091, 3096.
(7) Stockmayer, W. H. *J. Chem. Phys.* **1943**, *11*, 45; **1944**, *12*, 125.
(8) De Gennes, P.-G. *J. Phys. Lett.* **1976**, *37*, L1.
(9) Stauffer, D. *J. Chem. Soc., Faraday Trans. 2* **1976**, *72*, 1354.
(10) Flory P. J. *Principles of Polymer Chemistry*; Cornell University Press: Ithaca, NY, 1953.
(11) De Gennes, P. G. C. R. *Hebd. Séances Acad. Sci.* **1980**, *17*, 291.
(12) van Benthem, R. A. T. M.; Meijerink, N.; Geladé, E.; de Koster, C. G.; Muscat, D.; Froehling, P. E.; Hendriks, P. H. M.; Vermeulen, C..A. A.; Zwartkruis, J. G. *Macromolecules*, in press.
(13) (a) Flory, P. J. *J. Am. Chem. Soc.* **1952**, *74*, 2718. (b) Burchard, W. *Adv. Polym. Sci.* **1983**, *48*, 1.
(14) Hobson, L. J.; Harrison, R. M. *Curr. Opin. Solid State Mater. Sci.* **1997**, *2*, 683.
(15) Grubisic, Z.; Rempp, R.; Benoit, H. *J. Chim. Phys.* **1966**, *63*, 1507.
(16) Mourey, T. H.; Turner, S. R.; Rubinstein, M.; Fréchet, J. M. J.; Hawker, C. J.; Wooley, K. L. *Macromolecules* **1992**, *25*, 2401.
(17) Patton, E. V.; Wesson, J. A.; Rubinstein, M.; Wilson, J. C.; Oppenheimer, L. E. *Macromolecules* **1989**, *22*, 1946.
(18) Kim, Y. H.; Webster, O. In *Star and hyperbranched polymers*; Mishra, M. K., Kobayashi, S., Ed.; Marcel Dekker Inc.: New York, 1999; Chapter 8, p 201
(19) Voit, B. I. *Acta Polym.* **1995**, *46*, 87.
(20) Nielen, M. W. F. *Mass Spectrom. Rev.* **1999**, *18*, 309.
(21) (a) Prosa, Ty J.; Bauer, B. J.; Amis, E. J.; Tomalia, D. A.; Scherrenberg, R. *J. Polym. Sci., Part B: Polym. Phys.* **1997**, *35*, 2913. (b) Bauer, B. J.; Topp, A.; Prosa, Ty J.; Amis, E. J.; Yin, R.; Qin, D.; Tomalia, D. A. *Polym. Mater. Sci. Eng.* **1997**, *77*, 87.
(22) Vestal, M. L.; Juhasz, P.; Martin, S. A. *Rapid Commun. Mass Spectrom.* **1995**, *9*, 1044.
(23) van Benthem, R. A. T. M.; de Koster, C. G.; Fokkens, R.; Nibbering, N. M. M. *J. Am. Soc. Mass Spectrom.* **2000**, *11*, 218.
(24) Van Rooij, G. J.; Duursma, M. C.; Heeren, R. M. A.; Boon, J. J.; de Koster, C. G. *J. Am. Soc. Mass Spectrom.* **1996**, *7*, 449.
(25) De Koster, C. G.; Duursma, M. C.; van Rooij, G. J.; Heer, R. M.; Boon, J. J. *Rapid Commun. Mass Spectrom.* **1995**, *9*, 957.
(26) Guinier, A.; Fournet, G. *Small Angle Scattering of X-rays*; Wiley: New York, 1955.
(27) Glatter, O.; Kratky, O. *Small Angle Scattering*; Academic Press: New York, 1982.
(28) Higgins, J. S.; Benoit, H. C. *Polymers and Neutron Scattering*; Claredon Press: Oxford, England, 1994.
(29) Richards, E. G. *An introduction to physical properties of large molecules in solution*; Cambridge University Press: New York, 1980.
(30) Martin, J. E.; Hurd, A. J. *J. Appl. Crystallogr.* **1987**, *20*, 61.
(31) Mandelbrot, B. B. *The Fractal Geometry of Nature*; W. H. Freeman, San Francisco, CA, 1982.
(32) Scherrenberg, R.; Coussens, B.; van Vliet, P.; Edouard, G.; Brackman, J.; de Brabander, E. *Macromolecules* **1998**, *31*, 456.
(33) Burchard, W. *Adv. Polym. Sci.* **1999**, *143*, 113.
(34) Daoud, M.; Family, F.; Jannink, J. *J. Phys. Lett.* **1984**, *45*, L199.
(35) Stauffer, D. *Introduction to percolation theory*; Taylor & Francis: London, 1985.
(36) Stauffer, D.; Coniglio, A.; Adam, M. *Adv. Polym. Sci.* **1982**, *44*, 103.
(37) Leibler, L.; Schosseler, F. *Phys. Rev. Lett.* **1985**, *55*, 1110.
(38) Colby, R. H.; Rubinstein, M.; Gillmor, J. R.; Mourey, T. H. *Macromolecules* **1992**, *25*, 7180.
(39) Hamielec, A. E.; Ouano, A. C. *J. Liq. Chromatogr.* **1978**, *1* (1), 1978.
(40) Jahromi, S.; Coussens, B.; Meijerink, N.; Braam, A. W. M. *J. Am. Chem. Soc.* **1998**, *120*, 9753.

MA001266T